

## A tutorial on mixed-domain wave-equation migration and migration velocity analysis

Paul Sava<sup>1</sup>

### ABSTRACT

This tutorial describes mixed-domain wave-equation migration and migration velocity analysis techniques in a unified theoretical framework. I review two of the most general mixed-domain migration methods, Fourier finite-difference and generalized screen, and show how other commonly used wave-equation migration methods come about as special cases. I use the Born approximation to derive general expressions for the wave-equation migration velocity analysis operator, and show two simple backprojection examples built around a North Sea dataset.

### INTRODUCTION

Wave-equation migration velocity analysis, WEMVA, (Biondi and Sava, 1999; Sava and Biondi, 2000) is a new and promising imaging tool, specifically aimed at regions of high geological complexity. The WEMVA method operates through recursive migration of the data, with the goal of improving the quality of the migrated images. Consequently, the operator used for WEMVA is tightly coupled with the operators used for migration, therefore a good understanding of the WEMVA operator requires a similar understanding of the migration operators from which it is derived.

The main goal of this paper is to clarify the theoretical origins of the WEMVA method, and to precisely show how it relates to the larger family of migration methods from which it is derived, the *mixed-domain* migration methods.

I begin with a review of mixed-domain migration. The two most general members of the family are known in the literature as the *Fourier finite-difference* (FFD) method, introduced by Ristow and Ruhl (1994), and the *generalized screen* (GSP) method (de Hoop, 1996). All the other methods in the family are just simplified cases, where we neglect some of the terms of the general relations. We can easily find many other methods known in the literature under various names, like: phase-shift (Gazdag, 1978; Gazdag and Sguazzero, 1984), split-step Fourier (Stoffa et al., 1990), local Born-Fourier or pseudo-screen (Huang and Wu, 1996), complexified pseudo-screen (de Hoop and Wu, 1996), extended local Born-Fourier (Huang et al., 1999), a.s.o. Here, I present all these methods in a unified framework, with the goal of facilitating easy navigation through the relevant literature.

---

<sup>1</sup>email: paul@sep.stanford.edu

Next, I generalize the WEMVA operator based on the mixed-domain operators from which it is derived. It turns out that a Born linearization of either the FFD or the GSP relations, give general expressions for the WEMVA operator, from which we can obtain various special cases, as it is done for the associated mixed-domain migration methods.

Finally, I use a North Sea example to visualize the results of the WEMVA backprojection operator. I simulate small, localized perturbations on the seismic image, and show how they get backprojected in the slowness function using a particular choice of the WEMVA operator. The result is a bundle of “fat” rays, which can be correlated with the trajectories obtained for rays built using conventional ray tracing. This comparison enables us to easily visualize the band-limited character of wave-equation migration velocity analysis, and to gain insight into how this method operates in a real case.

Next section presents the general mixed-domain migration equations, followed by a discussion of the Born approximation and two sections dedicated to the various approximations encountered in the literature. In the end, I show how we can generalize the scattering and, implicitly, the WEMVA operators, and finish with the example on the North Sea dataset.

## MIXED-DOMAIN MIGRATION THEORY

Downward continuation is the process in which we recursively extrapolate in depth the wavefield recorded at the surface. Mathematically, this operation amounts to a phase shift applied to the wavefield (Claerbout, 1985)

$$U_{z+\Delta z} = \mathcal{T}U_z,$$

where  $U_z$  is the wavefield at depth  $z$ , and  $U_{z+\Delta z}$  is the extrapolated wavefield at depth  $z + \Delta z$ . The downward continuation operator at depth  $z$  is

$$\mathcal{T} = e^{ik_z \Delta z}, \quad (1)$$

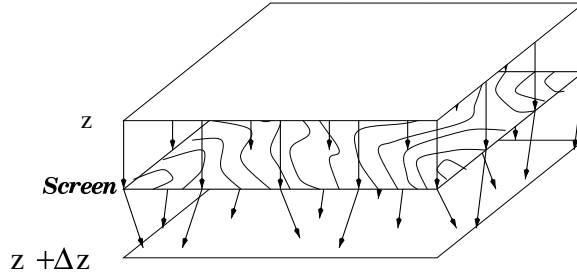
with the vertical wavenumber,  $k_z$ , given by the one-way wave equation, also known as the single square root (SSR) equation

$$k_z = \sqrt{\omega^2 s^2 - |\mathbf{k}_m|^2},$$

where  $\omega$  is the temporal frequency,  $s$  is the laterally variable slowness of the medium, and  $\mathbf{k}_m$  is the horizontal wavenumber.

Since downward continuation by phase shift can be applied for slowness models that only vary with depth, we need to split the operator  $\mathcal{T}$  into two parts: a constant slowness *continuation operator* applied in the  $\omega - \mathbf{k}$  domain, which accounts for the propagation in depth, and a *screen operator* applied in the  $\omega - \mathbf{x}$  domain, which accounts for the wavefield perturbations due to the lateral slowness variations. In essence, we approximate the vertical wavenumber  $k_z$  with its constant slowness counterpart  $k_{z_0}$ , corrected by a term describing the spatial variability of the slowness function (Figure 1).

Figure 1: A sketch of mixed-domain migration. The wavefield at depth  $z$  is downward continued to depth  $z + \Delta z$  through a variable-slowness screen. paul1-screen [NR]



### Fourier finite-difference

In one of its most general forms (Ristow and Ruhl, 1994), we can write  $k_z$  as

$$k_z = k_{z_o} + \omega \left[ 1 - \frac{s}{s_o} \left( \sum_{n=1}^{\infty} (-1)^n \binom{\frac{1}{2}}{n} \left[ \frac{|\mathbf{k}_m|}{\omega s} \right]^{2n} \delta_n \right) \right] (s - s_o), \quad (2)$$

where  $\binom{\frac{1}{2}}{n}$  are binomial coefficients for integer numbers  $n$ ,  $s$  represents the spatially variable slowness function at depth  $z$ ,  $s_o$  is a constant approximation to  $s$ , and  $\delta_n$  is a sum of terms derived from  $s$  and  $s_o$ . The FFD equation is obtained using two Taylor series expansions of the SSR equations written for  $k_z$  and  $k_{z_o}$ . I give a full derivation of Equation (2) in Appendix A.

Higher accuracy can be achieved by replacing the Taylor expansion in Equation (2) with Muir's continuous fraction expansion (Claerbout, 1985). The equivalent form of the general Fourier finite-difference propagator is:

$$k_z = k_{z_o} + \omega \left[ 1 - \frac{s}{s_o} \left( \sum_{n=1}^{\infty} \frac{\left[ \frac{|\mathbf{k}_m|}{\omega s} \right]^2}{a_n + b_n \left[ \frac{|\mathbf{k}_m|}{\omega s} \right]^2} \right) \right] (s - s_o), \quad (3)$$

where  $a_n$  and  $b_n$  are coefficients that, in general, depend on the medium and the constant reference slownesses,  $s$  and  $s_o$ . The coefficients  $a_n$  and  $b_n$  are derived either by identification of terms between Equation (2) and Equation (3), after the approximation  $\frac{1}{1-x^2} \approx 1 + x^2$ , or by an optimization problem as described by Ristow and Ruhl (1997).

### Generalized screen

In a second general form, given by the generalized screen propagator (GSP) (Le Rousseau and de Hoop, 1998), we can write  $k_z$  as

$$k_z = k_{z_o} + k_{z_o} \sum_{n=1}^{\infty} (-1)^n \binom{\frac{1}{2}}{n} \left[ \left( \frac{\omega^2 s_o^2}{\omega^2 s_o^2 - |\mathbf{k}_m|^2} \right) \left( \frac{s_o^2 - s^2}{s_o^2} \right) \right]^n. \quad (4)$$

The GSP equation is obtained through a Taylor series expansion of  $k_z$ , assuming small variations between the true ( $s$ ) and reference ( $s_o$ ) slownesses. A full derivation of Equation (4) is given in Appendix B.

Equation (4) may become unstable when the denominator of the sum vanishes. One way to avoid such a situation is to replace the vanishing term with another Taylor series expansion

$$k_z = k_{z_o} + k_{z_o} \sum_{n=1}^{\infty} (-1)^n \binom{\frac{1}{2}}{n} \left[ \left( \sum_{i=0}^{\infty} (-1)^i \binom{-1}{i} \left[ \frac{|\mathbf{k}_m|^2}{(\omega s_o)^2} \right]^i \right) \left( \frac{s_o^2 - s^2}{s_o^2} \right) \right]^n. \quad (5)$$

As for the FFD equation, we can achieve higher accuracy by replacing the Taylor series expansions with Muir's continuous fraction expansions.

We can use Equations (2) and (5) to derive the formulae for many of the methods commonly referred to as screen propagators, using various approximations for the vertical wavenumber  $k_z$ . For simplicity, however, in the next sections I use the Fourier finite-difference equation (2), because it offers a much more straight-forward derivation of the simplified cases, together with easier implementation. Nevertheless, Equation (5) can also be used to obtain the simplified cases, as presented in Appendix B.

Figure 2 is a comparison of the angular accuracy achieved by the two methods, FFD and GSP. GSP achieves higher angular accuracy compared to FFD for the same order of the approximation, although, as mentioned earlier, stability requires further approximations that inevitably decrease the accuracy of GSP. Furthermore, the GSP equation involves  $k_{z_o}$  in the Taylor series expansion, which does not have a straightforward finite-difference implementation.

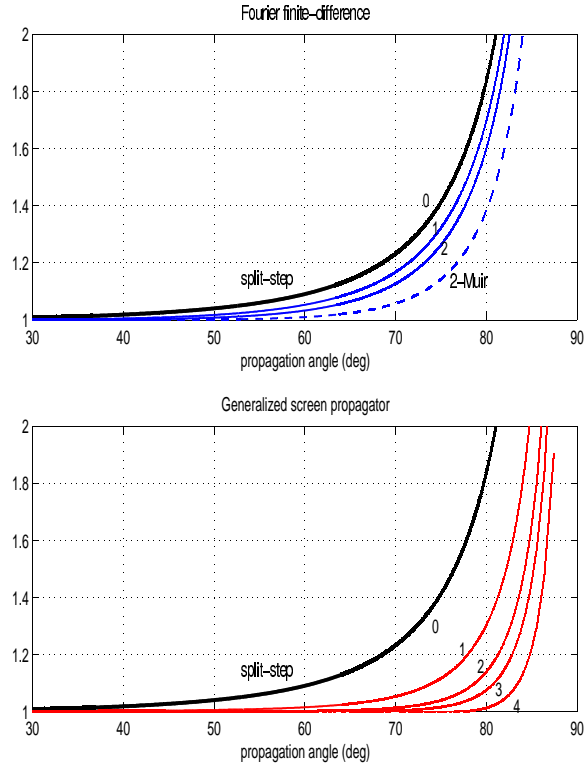
## BORN APPROXIMATION

Equation (1) exhibits a non-linear relationship between the laterally variable slowness and the propagated wavefield. For the remaining of this paper, I will conventionally refer to the methods in this class as non-linear methods. A second class of methods are found using the Born approximation for the wavefield perturbations. In physical terms, this approximation is only valid for media characterized by weak scattering, that is small velocity variation. Mathematically, the Born approximation is equivalent to a linearization of the exponential  $e^x \approx 1 + x$ . With this new approximation, the expression for the downward-continued wavefield becomes:

$$U_{z+\Delta z} \approx e^{ik_{z_o}\Delta z} U_z \left\{ 1 + i\Delta z\omega \left[ 1 - \frac{s}{s_o} \left( \sum_{n=1}^{\infty} (-1)^n \binom{\frac{1}{2}}{n} \left[ \frac{|\mathbf{k}_m|}{\omega s} \right]^{2n} \delta_n \right) \right] (s - s_o) \right\}. \quad (6)$$

Next two sections describe the various mixed-domain methods belonging to the two aforementioned classes, linear and non-linear, in relation to the general formula given by Equation (2).

Figure 2: Angular accuracy comparison between FFD and GSP. The horizontal axis is the propagation angle, while the vertical axis is the ratio of the approximate and true values of the depth wavenumbers. Various curves correspond to different levels of accuracy. The thicker line corresponds to the split-step Fourier method. The dashed line corresponds to FFD using a second order Muir continuous fraction expansion. For both FFD and GSP, the higher order approximations achieve higher accuracy. The graphs correspond to  $1/s = 2.0$  km/s and  $1/s_o = 1.9$  km/s. `paul1-ffdgsp` [CR]



## NON-LINEAR MIGRATION METHODS

The non-linear class of methods preserve the downward continuation operator, given by Equation (1), in its exponential form. Starting from Equation (2), we can derive the equations that describe various approximate migration methods. Here is a summary of methods, going from complex to simple:

1. We can simplify the FFD migration equation by ignoring the spatial variability of the slowness function for the terms of the summation,  $\frac{s}{s_o} = 1$  and  $\delta_n = \sum_{\substack{l=0 \\ n \geq 1}}^{2n-2} 1$ , which gives the following equation (Biondi, 1999):

$$k_z \approx k_{z_o} + \omega \left[ 1 - \left( \sum_{n=1}^{\infty} (-1)^n \binom{\frac{1}{2}}{n} \left[ \frac{|\mathbf{k}_m|}{\omega s_o} \right]^{2n} (2n-1) \right) \right] (s - s_o). \quad (7)$$

2. In the next simplification, we consider, in addition to the earlier approximations, that the ratio  $\frac{s}{s_o} = 0$ , which leads to the *split-step Fourier* method a.k.a. *phase-screen* method (Stoffa et al., 1990):

$$k_z \approx k_{z_o} + \omega(s - s_o) \quad (8)$$

3. Finally, the simplest method of the family is *phase-shift* (Gazdag, 1978; Gazdag and Sguazzero, 1984), for which we further assume that  $s - s_o = 0$ , therefore

$$k_z \approx k_{z_o}. \quad (9)$$

For most of these methods, we can separate approximations of various *orders*, depending on the number of terms in the sum ( $n$ ). We can also have versions that use several values of the reference slowness ( $s_o$ ), followed by *interpolation* of the continued wavefield.

The bottom line is that all these simplified methods are just particular cases of the *Fourier finite-difference* method mathematically described by Equation (2). Similarly, we can derive all these simplified methods from the *generalized screen* method, mathematically described by Equation (5).

## LINEAR MIGRATION METHODS

Another class of screen methods are derived using the Born approximation applied to the scattered wavefield. Mathematically, this is described by a linearization of the downward continuation operator. After linearization, the wavefield at depth  $z + \Delta z$  is related to the wavefield at the previous depth level  $z$  by Equation (6). As for the non-linear methods, we can simplify this equation, and obtain different methods commonly encountered in the literature:

1. We can, again, ignore the spatial variability of the slowness function for the terms of the summation,  $\frac{s}{s_o} = 1$  and  $\delta_n = \sum_{\substack{l=0 \\ n \geq 1}}^{2n-2} 1$ , which gives the following linear mixed-domain migration equation, known in the literature as the *extended local Born-Fourier* method (Huang et al., 1999):

$$U_{z+\Delta z} \approx e^{ik_{z_o}\Delta z} U_z \left\{ 1 + i \Delta z \omega \left[ 1 - \left( \sum_{n=1}^{\infty} (-1)^n \binom{\frac{1}{2}}{n} \left[ \frac{|\mathbf{k}_m|}{\omega s_o} \right]^{2n} (2n-1) \right) \right] (s - s_o) \right\}. \quad (10)$$

2. We can consider Equation (10) as a Taylor series expansion, therefore we can write it in a more compact, but equivalent, form as

$$U_{z+\Delta z} \approx e^{ik_{z_o}\Delta z} U_z \left[ 1 + i \Delta z \omega \frac{\omega s_o}{\sqrt{\omega^2 s_o^2 - |\mathbf{k}_m|^2}} (s - s_o) \right]. \quad (11)$$

This equation describes the *local Born-Fourier* a.k.a. *pseudo-screen* method (Huang and Wu, 1996).

The extended local Born-Fourier method, Equation (10), is preferable in practice, since Equation (11) can lead to instability when the denominator vanishes. Another way of avoiding the instability is to add a small complex quantity,  $i\eta |\mathbf{k}_m|$ , to the denominator,

method that is known as the *complexified local Born-Fourier* or *complexified pseudo-screen* method (de Hoop and Wu, 1996):

$$U_{z+\Delta z} \approx e^{ik_{z_o}\Delta z} U_z \left[ 1 + i\Delta z\omega \frac{\omega s_o}{\sqrt{\omega^2 s_o^2 - (1-i\eta)^2 |\mathbf{k}_m|^2}} (s - s_o) \right] \quad (12)$$

### SCATTERING AND MIGRATION VELOCITY ANALYSIS

The generalization analyzed in the preceding sections can also be used in the area of wave-equation migration velocity analysis (Biondi and Sava, 1999; Sava and Biondi, 2000).

The downward continued wavefield in Equation (6) can be rewritten as

$$U_{z+\Delta z} = \mathcal{T} U_z \{1 + \mathcal{S}(s - s_o)\} \quad (13)$$

where, as before,  $\mathcal{T}$  is the downward continuation operator applied in the  $\omega - \mathbf{k}$  domain, and  $\mathcal{S}$  is the scattering operator, applied in the  $\omega - \mathbf{x}$  domain. The scattered wavefield created at depth  $z + \Delta z$  under the influence of the background wavefield ( $U_z$ ) by a slowness perturbation at depth  $z$  ( $\Delta s_z = s - s_o$ ) is

$$\Delta W_{z+\Delta z} = \mathcal{T} U_z \mathcal{S} \Delta s_z, \quad (14)$$

where the general form of the scattering operator derived from FFD is

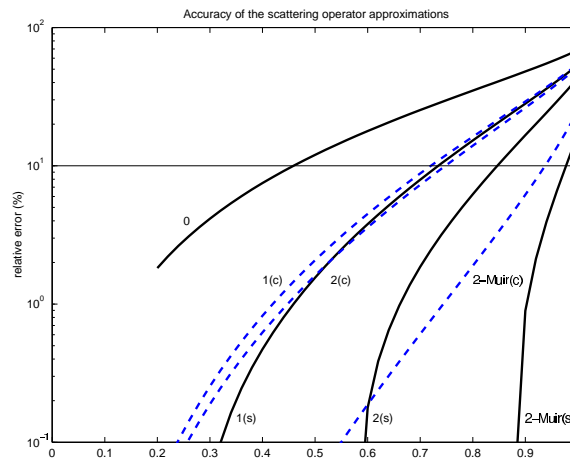
$$\mathcal{S} = i\Delta z\omega \left[ 1 - \frac{s}{s_o} \left( \sum_{n=1}^{\infty} (-1)^n \binom{\frac{1}{2}}{n} \left[ \frac{|\mathbf{k}_m|}{\omega s} \right]^{2n} \delta_n \right) \right]. \quad (15)$$

When computed using the operator in Equation (15), the scattered wavefield, Equation (14), exhibits a nonlinear relation to the slowness perturbation. A straightforward linearization is to approximate  $\mathcal{S}$  for the constant background slowness. Biondi and Sava (1999) implement the prestack version of the scattering operator using a 4<sup>th</sup> order Taylor series expansion, under the constant velocity assumption ( $\delta_n = 2n - 1$  and  $s = s_o$ ) for all the terms in the sum:

$$\mathcal{S} \approx i\Delta z\omega \left( 1 + \frac{1}{2} \left[ \frac{|\mathbf{k}_m|}{\omega s_o} \right]^2 + \frac{3}{8} \left[ \frac{|\mathbf{k}_m|}{\omega s_o} \right]^4 + \frac{5}{16} \left[ \frac{|\mathbf{k}_m|}{\omega s_o} \right]^6 + \frac{35}{128} \left[ \frac{|\mathbf{k}_m|}{\omega s_o} \right]^8 \right). \quad (16)$$

Figure 3 shows a comparison of various approximation for the linear scattering operator, Equation (15). As expected, the relative error of the backprojection operator increases with increasing ratio  $\left[ \frac{|\mathbf{k}_m|}{\omega s} \right]$ . Also, Muir's continuous fraction expansion gives a significantly better approximation to the scattering operator for the same order of the expansion. The solid horizontal line corresponds to 10% relative error of the approximate to the true scattering operator.

Figure 3: Comparison of various approximation for the linear scattering operator. The solid lines correspond to scattering operators computed using the spatially variable slowness function ( $s$ ), and the dashed lines correspond to the scattering operator computed using only the background slowness ( $s_o$ ). The accuracy of the operator improves when using the variable slowness function. The horizontal axis is the ratio  $\left[\frac{|k_m|}{\omega s}\right]$ , and the vertical axis is the relative error of the linear scattering operator with respect to the true one, in logarithmic scale. paul1-sc [CR]



After we apply the imaging condition to the downward continued scattered wavefield Equation (13), we can formulate the relationship between the image ( $\Delta\mathbf{R}$ ) and slowness ( $\Delta\mathbf{S}$ ) perturbations as

$$\Delta\mathbf{R} \approx \mathcal{L}\Delta\mathbf{S} \quad (17)$$

where  $\mathcal{L}$  is the wave-equation migration velocity analysis operator (Biondi and Sava, 1999).

Next section presents a simple example, in which I simulate  $\Delta\mathbf{R}$  and compute  $\Delta\mathbf{S}$  using a prestack backprojection operator derived from Equation (16).

## WEMVA EXAMPLES

I exemplify the simple application of the backprojection operator in Equation (17) on a North Sea dataset (Vaillant and Sava, 1999; Sava, 2000). Figure 4 is the velocity map used to compute the background wavefield, and Figure 5 is the image obtained after split-step migration with the background slowness model using three reference velocities.

The image is extracted from common-image gathers at a selected value of the offset ray-parameter (Prucha et al., 1999), which is approximately equivalent to the image for a given incidence angle at the reflectors (Sava and Fomel, 2000). As expected, the geologic structure is not perfectly defined by one single incidence angle, although this is not a problem for these examples, since I use the image at a given incidence angle only to create the image perturbation, but use the entire prestack image as background during backprojection.

Figure 6 is a simulated image perturbation ( $\Delta\mathbf{R}$ ) localized under the salt flank. I create this perturbation by cutting a small window in the target region, shifting it down so that the



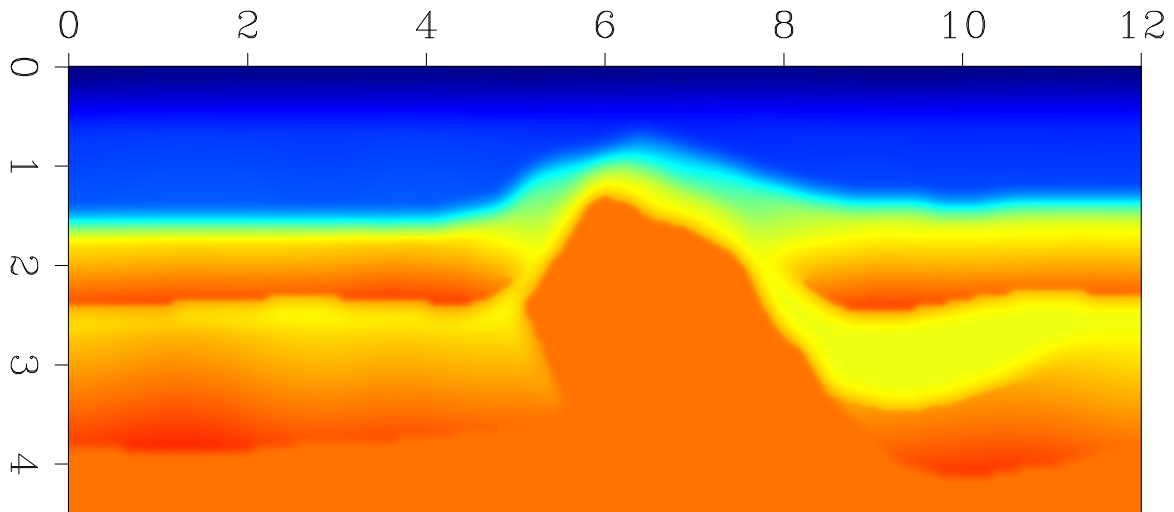


Figure 4: Velocity map for the North Sea dataset. `paul1-fat.V` [CR]

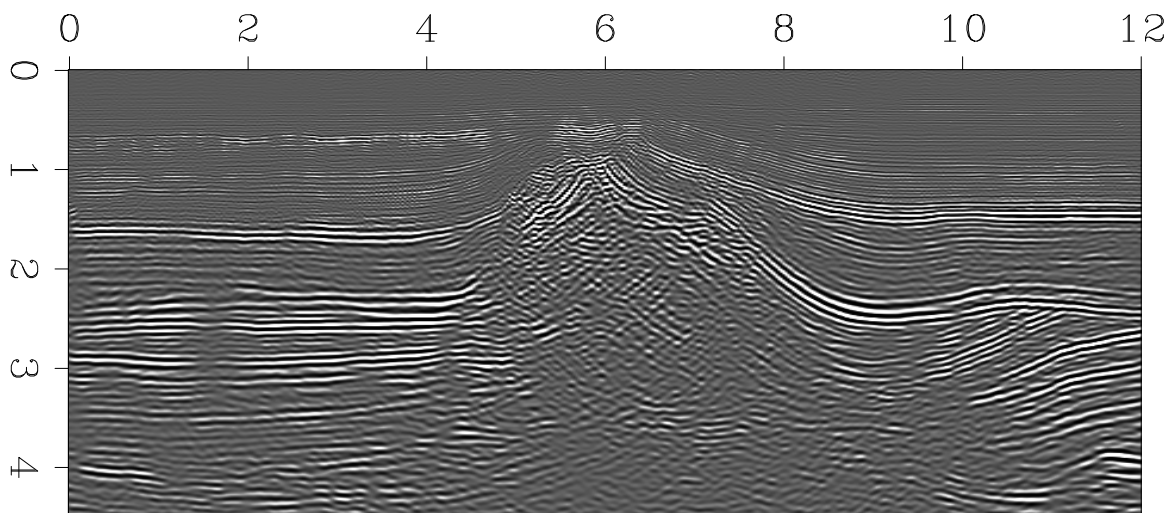


Figure 5: The image at a selected offset ray parameter. `paul1-fat.R` [CR]

phase difference between the two images doesn't violate the Born approximation, and taking the difference.

Next, Figure 7 is the result of applying the backprojection operator in Equation (17) to the image perturbation in Figure 6. The backprojection operator turns the image perturbation into a bundle of "fat" rays ( $\Delta\mathbf{S}$ ) emerging from the region of perturbation. The rays follow various trajectories, in accordance to the velocity model and with the background image.

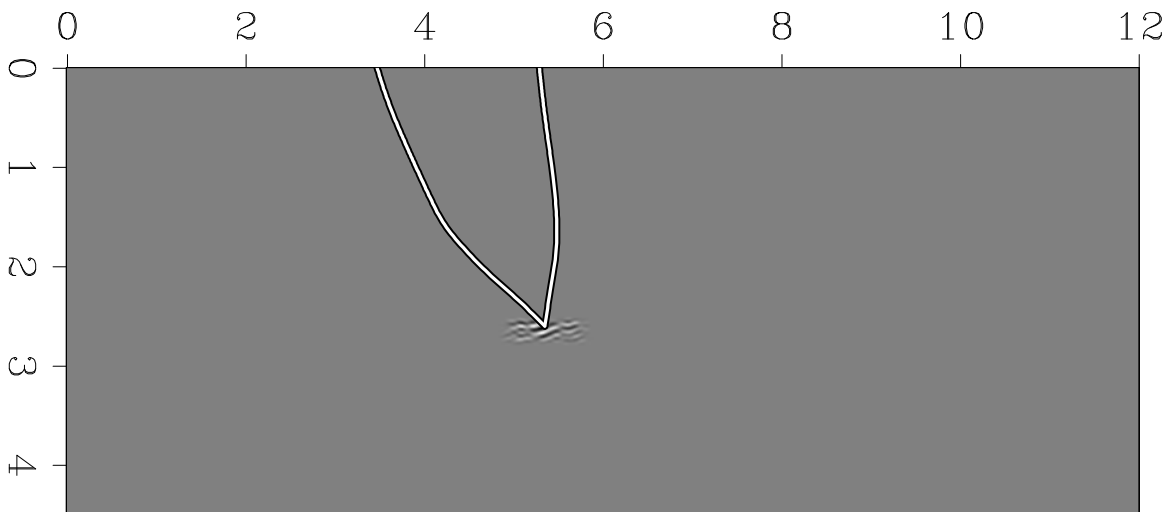


Figure 6: Image perturbation situated under the salt flank, overlaid by a pair of specular rays. `paul1-fat.DR3` [CR]

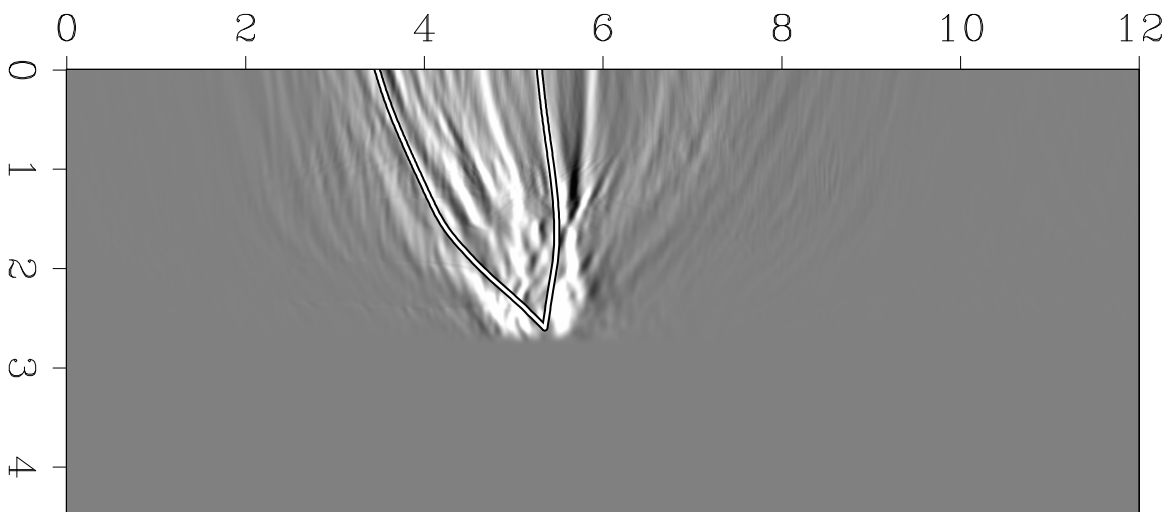


Figure 7: Slowness perturbation obtained by backprojecting the image perturbation in Figure 6. Overlaid are a pair of specular rays. `paul1-fat.DS3` [CR]

For comparison, I superimpose on both images in Figures 6 and 7 a pair of specular rays, shot at roughly the same angle with respect to the normal to a hypothetical reflector in the

perturbation region as the angle given by the offset ray parameter at which I selected the image perturbation. The rays overlap well over one pair of “fat” rays. In fact, these images graphically illustrate the band-limited character of wave-equation migration velocity analysis, which is its most important property.

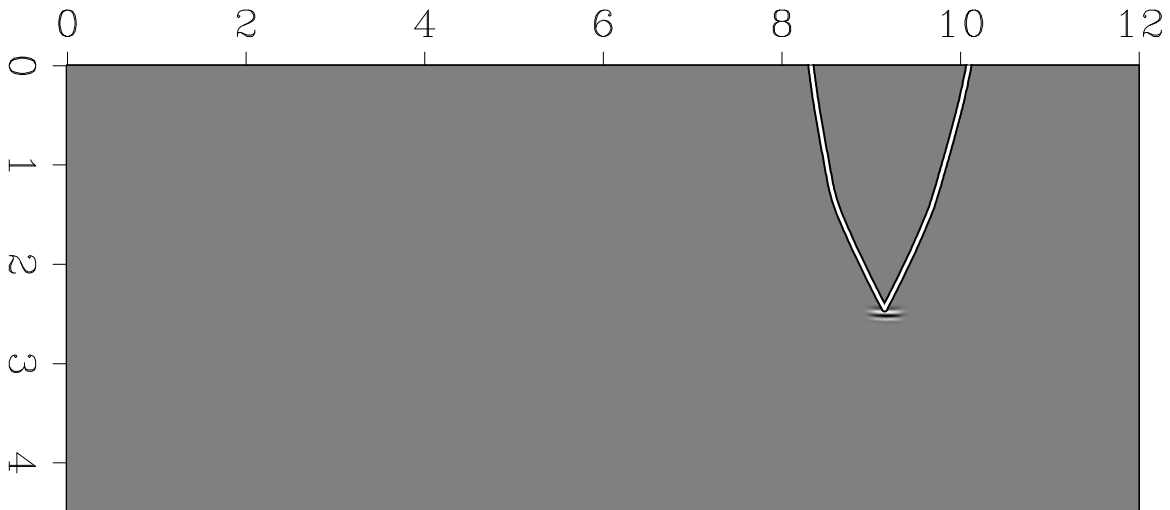


Figure 8: Image perturbation situated away from the salt flank, overlaid by a pair of specular rays. `paul1-fat.DR4` [CR]

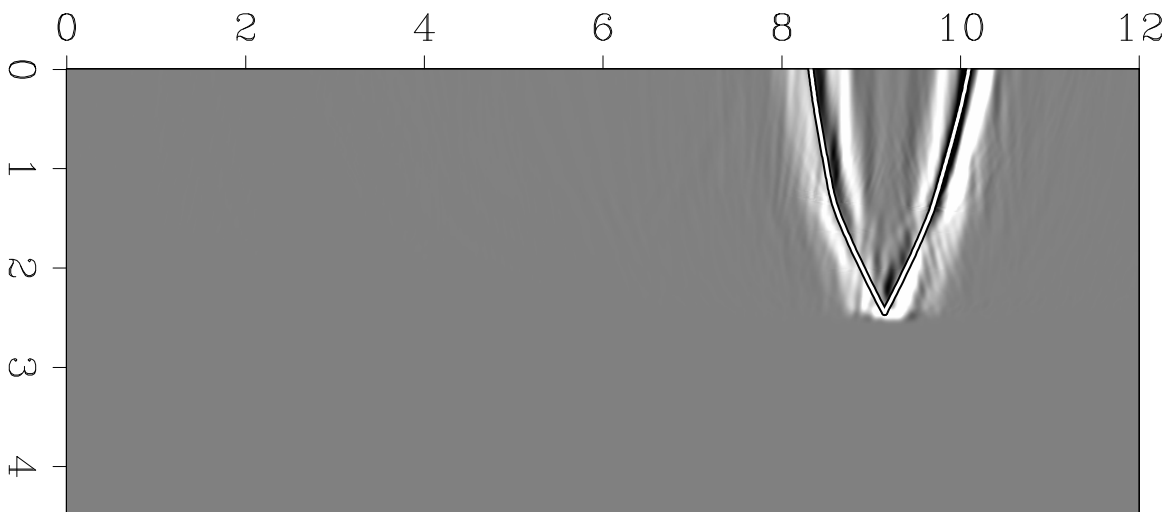


Figure 9: Slowness perturbation obtained by backprojecting the image perturbation in Figure 8. Overlaid are a pair of specular rays. `paul1-fat.DS4` [CR]

The backprojection in Figure 7 corresponds to just a particular selection of the incidence angle at the reflector. Perturbations at other angles backproject over other regions of the slowness model. When all backprojections are put together, we obtain a smoother version of slowness perturbation in comparison to that obtained using ray tomography (Sava and

Biondi, 2000). Ray tomography requires a significant amount of model regularization (Clapp and Biondi, 1999) to control the shape of the inverted model. However, given its intrinsic band-limited nature, wave-equation migration velocity analysis requires less regularization, or model-styling, applied on the slowness model. The net result is that we need less a-priori information about our slowness model, and we can extract more information from our data.

Unlike in the first example, Figures 6 and 7, where part of the wavefield propagates through the salt and, therefore, some of the fat rays get significantly distorted, in a second example the wavefield propagates through a much simpler part of the velocity model, and so the fat rays are less distorted (Figures 8 and 9).

As pointed out by Sava and Biondi (2000), the Born approximation is the biggest limitation of the method, since stability requires us to ensure that we do not violate the small-perturbation assumption. Also, the frequency content of the images is not the same, therefore we can obey the Born approximation in some regions, but violate it in others. Better ways to control the Born approximation await for future research.

## CONCLUSION

Fourier finite-difference (FFD) and generalized screen (GSP) are two of the most general members of the mixed-domain wave-equation migration family. For the same order of approximation, GSP can achieve a higher angular accuracy than FFD, although GSP's implementation is not as straightforward as that of FFD, and its stability is harder to ensure. Other members of the family can be easily obtained by simply neglecting some of the terms in the general equations. This paper serves as a tutorial that brings together all the members of the family in a unified framework.

By analogy with mixed-domain migration operators, I generalize the wave-equation migration velocity analysis operator. Many other approximate formulae can be derived from the general WEMVA equations. The approximations with the largest impact are those based only on the background slowness, which enable linearized image perturbation – slowness perturbation relationship.

Simple backprojection examples illustrate the band-limited character of velocity analysis using the wave-equation. I present WEMVA “fat” rays that are easy to correlate to high-frequency trajectories obtained by conventional ray-tracing.

## ACKNOWLEDGEMENT

Biondi Biondi suggested the fat rays analysis and the North Sea example used in this paper.

## REFERENCES

Biondi, B., and Sava, P., 1999, Wave-equation migration velocity analysis: SEP-100, 11–34.

- Biondi, B. L., 1999, 3-D Seismic Imaging: Stanford Exploration Project.
- Claerbout, J. F., 1985, *Imaging the Earth's Interior*: Blackwell Scientific Publications.
- Clapp, R. G., and Biondi, B., 1999, Preconditioning tau tomography with geologic constraints: SEP-**100**, 35–50.
- de Hoop, M. V., and Wu, R. S., 1996, General formulation of screen methods for the scattering of waves in inhomogeneous media: *Wave Motion*, submitted.
- de Hoop, M. V., 1996, Generalization of the Bremmer coupling series: *J. Math. Phys.*, 3246–3282.
- Gazdag, J., and Sguazzero, P., 1984, Migration of seismic data by phase-shift plus interpolation: *Geophysics*, **49**, no. 2, 124–131.
- Gazdag, J., 1978, Wave equation migration with the phase-shift method: *Geophysics*, **43**, no. 7, 1342–1351.
- Huang, L.-J., and Wu, R.-S., 1996, 3-D prestack depth migration with acoustic pseudo-screen propagators *in* Hassanzadeh, S., Ed., *Mathematical methods in geophysical imaging IV*:: Proc. SPIE: The International Society for Optical Engineering, 40–51.
- Huang, L., Fehler, M. C., and Wu, R. S., 1999, Extended local Born Fourier migration method: *Geophysics*, **64**, no. 5, 1524–1534.
- Le Rousseau, J., and de Hoop, M., 1998, Modeling and imaging with the generalized screen algorithm: 68th Ann. Internat. Meeting, Soc. Expl. Geophys., 1937–1940.
- Prucha, M. L., Biondi, B. L., and Symes, W. W., 1999, Angle-domain common image gathers by wave-equation migration: SEP-**100**, 101–112.
- Ristow, D., and Ruhl, T., 1994, Fourier finite-difference migration: *Geophysics*, **59**, no. 12, 1882–1893.
- Ristow, D., and Ruhl, T., 1997, 3-D implicit finite-difference migration by multiway splitting: *Geophysics*, **62**, no. 02, 554–567.
- Sava, P., and Biondi, B., 2000, Wave-equation migration velocity analysis: Episode II: SEP-**103**, 19–47.
- Sava, P., and Fomel, S., 2000, Angle-gathers by Fourier Transform: SEP-**103**, 119–130.
- Sava, P., 2000, Variable-velocity prestack Stolt residual migration with application to a North Sea dataset: SEP-**103**, 147–157.
- Stoffa, P. L., Fokkema, J. T., de Luna Freire, R. M., and Kessinger, W. P., 1990, Split-step Fourier migration: *Geophysics*, **55**, no. 4, 410–421.
- Vaillant, L., and Sava, P., 1999, Common-azimuth migration of a North Sea dataset: SEP-**102**, 1–14.

## APPENDIX A

This Appendix is a step-by-step derivation of the Fourier finite-difference equation, Equation (2), one of the most general forms of the equations describing mixed-domain migration.

I begin with Taylor series approximations of the single square root equations for the vertical wavenumbers corresponding to the true slowness ( $s$ )

$$k_z = \sqrt{\omega^2 s^2 - |\mathbf{k}_m|^2} = \omega s \sqrt{1 - \left[ \frac{|\mathbf{k}_m|}{\omega s} \right]^2} = \omega s \left[ 1 + \sum_{n=1}^{\infty} (-1)^n \binom{\frac{1}{2}}{n} \left[ \frac{|\mathbf{k}_m|}{\omega s} \right]^{2n} \right], \quad (\text{A-1})$$

and for the reference slowness ( $s_o$ )

$$k_{z_o} = \sqrt{\omega^2 s_o^2 - |\mathbf{k}_m|^2} = \omega s_o \sqrt{1 - \left[ \frac{|\mathbf{k}_m|}{\omega s_o} \right]^2} = \omega s_o \left[ 1 + \sum_{n=1}^{\infty} (-1)^n \binom{\frac{1}{2}}{n} \left[ \frac{|\mathbf{k}_m|}{\omega s_o} \right]^{2n} \right], \quad (\text{A-2})$$

where  $\binom{m}{n}$  are binomial coefficients <sup>2</sup> for real  $m$  and integer  $n$ . We can use Equation (A-2) to replace  $k_{z_o}$  in Equation (A-1) and obtain an equation relating the true depth wavenumber  $k_z$  to the reference one:

$$k_z = k_{z_o} + \omega(s - s_o) + \omega \sum_{n=1}^{\infty} (-1)^n \binom{\frac{1}{2}}{n} \left[ s \left[ \frac{|\mathbf{k}_m|}{\omega s} \right]^{2n} - s_o \left[ \frac{|\mathbf{k}_m|}{\omega s_o} \right]^{2n} \right]. \quad (\text{A-3})$$

Next we re-arrange the slowness terms of the equation to facilitate the substitution of the ratio of the true and reference slownesses:  $p = \frac{s}{s_o}$

$$k_z = k_{z_o} + \omega s_o \left( \frac{s}{s_o} - 1 \right) + \omega s_o \sum_{n=1}^{\infty} (-1)^n \binom{\frac{1}{2}}{n} \left[ \frac{|\mathbf{k}_m|}{\omega s} \right]^{2n} \left[ \frac{s}{s_o} - \frac{s^{2n}}{s_o^{2n}} \right], \quad (\text{A-4})$$

which leads to the more compact relation:

$$k_z = k_{z_o} + \omega s_o (p - 1) + \omega s_o \sum_{n=1}^{\infty} (-1)^n \binom{\frac{1}{2}}{n} \left[ \frac{|\mathbf{k}_m|}{\omega s} \right]^{2n} [p - p^{2n}]. \quad (\text{A-5})$$

If we make the change of variables

$$\delta_n = \sum_{\substack{l=0 \\ (n \geq 1)}}^{2n-2} p^l, \quad (\text{A-6})$$

we can write that

$$k_z = k_{z_o} + \omega s_o (p - 1) - \omega s_o (p - 1) p \sum_{n=1}^{\infty} (-1)^n \binom{\frac{1}{2}}{n} \left[ \frac{|\mathbf{k}_m|}{\omega s} \right]^{2n} \delta_n. \quad (\text{A-7})$$

---

<sup>2</sup>By definition,  $\binom{m}{n} = \frac{m(m-1)\dots(m-n+1)}{n!}$ .

Next, if we add and subtract  $\omega s_o p(p-1)$  on the right hand side of the preceding equation, we obtain that

$$k_z = k_{z_o} + \omega s_o(p-1) + \omega s_o p(p-1) - \omega s_o(p-1) p \sum_{n=0}^{\infty} (-1)^n \binom{\frac{1}{2}}{n} \left[ \frac{|\mathbf{k}_m|}{\omega s} \right]^{2n} \delta_n \quad (\text{A-8})$$

which can be simplified to

$$k_z = k_{z_o} + \omega s_o(p-1)(p+1) - \omega s_o(p-1) p \sum_{n=0}^{\infty} (-1)^n \binom{\frac{1}{2}}{n} \left[ \frac{|\mathbf{k}_m|}{\omega s} \right]^{2n} \delta_n, \quad (\text{A-9})$$

and, furthermore, to

$$k_z = k_{z_o} + \omega s_o(p-1) \left[ 1 + p \left( 1 - \sum_{n=0}^{\infty} (-1)^n \binom{\frac{1}{2}}{n} \left[ \frac{|\mathbf{k}_m|}{\omega s} \right]^{2n} \delta_n \right) \right], \quad (\text{A-10})$$

and, finally, to

$$k_z = k_{z_o} + \omega s_o(p-1) \left[ 1 - p \left( \sum_{n=1}^{\infty} (-1)^n \binom{\frac{1}{2}}{n} \left[ \frac{|\mathbf{k}_m|}{\omega s} \right]^{2n} \delta_n \right) \right]. \quad (\text{A-11})$$

If we make the reverse change of variables from  $p$  to  $s$  and  $s_o$ , we obtain the general Taylor expansion form of the depth wavenumber used for the FFD migration method:

$$k_z = k_{z_o} + \omega \left[ 1 - \frac{s}{s_o} \left( \sum_{n=1}^{\infty} (-1)^n \binom{\frac{1}{2}}{n} \left[ \frac{|\mathbf{k}_m|}{\omega s} \right]^{2n} \delta_n \right) \right] (s - s_o). \quad (\text{A-12})$$

The equivalent  $2^{nd}$  order equation takes the form:

$$k_z \approx k_{z_o} + \omega \left[ 1 + \frac{1}{2} \frac{1}{s s_o} \frac{|\mathbf{k}_m|^2}{\omega^2} + \frac{1}{8} \frac{1}{s s_o} \left( \frac{1}{s^2} + \frac{1}{s s_o} + \frac{1}{s_o^2} \right) \frac{|\mathbf{k}_m|^4}{\omega^4} \right] (s - s_o).$$

We can write an analogous form for Equation (A-12) using a continuous fraction expansion

$$k_z = k_{z_o} + \omega \left[ 1 - \frac{s}{s_o} \left( \sum_{n=1}^{\infty} \frac{\left[ \frac{|\mathbf{k}_m|}{\omega s} \right]^2}{a_n + b_n \left[ \frac{|\mathbf{k}_m|}{\omega s} \right]^2} \right) \right] (s - s_o). \quad (\text{A-13})$$

The equivalent  $2^{nd}$  order equation takes the form:

$$k_z \approx k_{z_o} + \omega \left[ 1 - \frac{\frac{1}{s s_o} \frac{|\mathbf{k}_m|^2}{\omega^2}}{-2 - \frac{1}{2} \left( \frac{1}{s^2} + \frac{1}{s s_o} + \frac{1}{s_o^2} \right) \frac{|\mathbf{k}_m|^2}{\omega^2}} \right] (s - s_o).$$

## APPENDIX B

This appendix is a step-by-step derivation of the generalized screen equation.

I begin with the single square root equation for the true slowness ( $s$ )

$$k_z = \sqrt{\omega^2 s^2 - |\mathbf{k}_m|^2},$$

and for the background slowness ( $s_o$ )

$$k_{z_o} = \sqrt{\omega^2 s_o^2 - |\mathbf{k}_m|^2}.$$

We can replace  $k_{z_o}$  in  $k_z$  to get

$$k_z = \sqrt{k_{z_o}^2 - \omega^2 (s_o^2 - s^2)}, \quad (\text{B-1})$$

or, in an equivalent form,

$$k_z = k_{z_o} \sqrt{1 - \frac{\omega^2 (s_o^2 - s^2)}{k_{z_o}^2}}.$$

Next, we can write a Taylor series expansion, assuming a small slowness squared perturbation  $s^2 - s_o^2$

$$k_z = k_{z_o} \sum_{n=0}^{\infty} (-1)^n \binom{\frac{1}{2}}{n} \left[ \frac{\omega^2 (s_o^2 - s^2)}{k_{z_o}^2} \right]^n.$$

The  $2^{nd}$  order approximation takes the form:

$$k_z = k_{z_o} - \frac{1}{2} \left[ \frac{\omega^2}{k_{z_o}} \right] (s_o^2 - s^2) - \frac{1}{8} \left[ \frac{\omega^2}{k_{z_o}} \right]^2 (s_o^2 - s^2)^2.$$

We can make  $k_{z_o}$  explicit for the terms of the sum and obtain

$$k_z = k_{z_o} \sum_{n=0}^{\infty} (-1)^n \binom{\frac{1}{2}}{n} \left[ \left( \frac{\omega^2 s_o^2}{\omega^2 s_o^2 - |\mathbf{k}_m|^2} \right) \left( \frac{s_o^2 - s^2}{s_o^2} \right) \right]^n, \quad (\text{B-2})$$

from which we can derive the generalized screen migration equation:

$$k_z = k_{z_o} + k_{z_o} \sum_{n=1}^{\infty} (-1)^n \binom{\frac{1}{2}}{n} \left[ \left( \frac{\omega^2 s_o^2}{\omega^2 s_o^2 - |\mathbf{k}_m|^2} \right) \left( \frac{s_o^2 - s^2}{s_o^2} \right) \right]^n. \quad (\text{B-3})$$

Because Equation (B-3) becomes unstable when the denominator of the terms in the summation vanishes, we replace these terms with another Taylor series expansion:

$$k_z = k_{z_o} + k_{z_o} \sum_{n=1}^{\infty} (-1)^n \binom{\frac{1}{2}}{n} \left[ \left( \sum_{i=0}^{\infty} (-1)^i \binom{-1}{i} \left[ \frac{|\mathbf{k}_m|^2}{(\omega s_o)^2} \right]^i \right) \left( \frac{s_o^2 - s^2}{s_o^2} \right) \right]^n. \quad (\text{B-4})$$



We can obtain the split-step equation through a sequence of approximations in Equation (B-4): first, we limit the terms of the inner Taylor series to two ( $i = 1, 2$ ) and the terms of the outer series to one ( $n = 1$ ), therefore

$$k_z \approx k_{z_o} + k_{z_o} \frac{-1}{2} \frac{(\omega s_o)^2}{k_{z_o}^2} \left(1 - \frac{s^2}{s_o^2}\right),$$

which we can simplify to

$$k_z \approx k_{z_o} - \frac{1}{2} \frac{\omega^2}{k_{z_o}} (s_o^2 - s^2).$$

Next, we approximate  $\frac{\omega}{k_{z_o}} \approx \frac{1}{s_o}$  and  $s_o + s \approx 2s_o$ , and get

$$k_z \approx k_{z_o} - \frac{1}{2s_o} 2s_o \omega (s_o - s).$$

which reduces to the split-step equation

$$k_z \approx k_{z_o} + \omega (s - s_o).$$

